Seasonal metabolism and carbon export potential of a key coastal habitat : The perennial canopy-forming macroalga Fucus vesiculosus

Attard, K. M.

2019-01

Attard , K M , Rodil , I F , Norkko , J , Norkko , A & Glud , R N 2019 , ' Seasonal metabolism and carbon export potential of a key coastal habitat : The perennial canopy-forming macroalga Fucus vesiculosus ' , Limnology and Oceanography , vol. 64 , no. 1 , pp. 149-164 . https://doi.org/10.1002/lno.11026 , https://doi.org/10.1002/lno.11026

http://hdl.handle.net/10138/298691
https://doi.org/10.1002/lno.11026

LIMNOLOGY
and
OCEANOGRAPHY

ASLO

Limnol. Oceanogr. 64, 2019, 149–164

doi: 10.1002/lno.11026

Seasonal metabolism and carbon export potential of a key coastal habitat: The perennial canopy-forming macroalga *Fucus vesiculosus*

K. M. Attard,[1,2*] I. F. Rodil,[1,3] P. Berg,[4] J. Norkko,[1] A. Norkko,[1,3] R. N. Glud[2,5]

[1]Tvärminne Zoological Station, University of Helsinki, Hanko, Finland
[2]Department of Biology, University of Southern Denmark, Odense, Denmark
[3]Baltic Sea Centre, Stockholm University, Stockholm, Sweden
[4]Department of Environmental Sciences, University of Virginia, Charlottesville, Virginia
[5]Department of Ocean and Environmental Sciences, Tokyo University of Marine Science and Technology, Tokyo, Japan

Abstract

The important role of macroalgal canopies in the oceanic carbon (C) cycle is increasingly being recognized, but direct assessments of community productivity remain scarce. We conducted a seasonal study on a sublittoral Baltic Sea canopy of the brown alga *Fucus vesiculosus*, a prominent species in temperate and Arctic waters. We investigated community production on hourly, daily, and seasonal timescales. Aquatic eddy covariance (AEC) oxygen flux measurements integrated ~ 40 m^2 of the seabed surface area and documented considerable oxygen production by the canopy year-round. High net oxygen production rates of up to 35 ± 9 mmol m^{-2} h^{-1} were measured under peak irradiance of ~ 1200 μmol photosynthetically active radiation (PAR) m^{-2} s^{-1} in summer. However, high rates > 15 mmol m^{-2} h^{-1} were also measured in late winter (March) under low light intensities < 250 μmol PAR m^{-2} s^{-1} and water temperatures of ~ 1°C. In some cases, hourly AEC fluxes documented an apparent release of oxygen by the canopy under dark conditions, which may be due to gas storage dynamics within internal air spaces of *F. vesiculosus*. Daily net ecosystem metabolism (*NEM*) was positive (net autotrophic) in all but one of the five measurement campaigns (December). A simple regression model predicted a net autotrophic canopy for two-thirds of the year, and annual canopy *NEM* amounted to 25 mol O_2 m^{-2} yr^{-1}, approximately six-fold higher than net phytoplankton production. Canopy C export was ~ 0.3 kg C m^{-2} yr^{-1}, comparable to canopy standing biomass in summer. Macroalgal canopies thus represent regions of intensified C assimilation and export in coastal waters.

Macroalgae form extensive canopies within near-shore areas that are among the most productive and biodiverse habitats on Earth (Mann 1973). Despite covering just ~ 7 million km^2, or < 2% of the total ocean area (Charpy-Roubad and Sournia 1990; Gattuso et al. 2006; Krause-Jensen and Duarte 2014), and accounting for < 5% of total oceanic net primary production (Field et al. 1998; Duarte 2017), macroalgal canopies represent "hotspots" of photosynthetic biomass. On a local scale, the biomass per unit area occupied by macroalgae can be approximately 400-fold greater than that of phytoplankton, and on a global scale, macrophyte biomass represents about two-thirds of total oceanic photosynthetic biomass (Smith 1981). Macroalgal beds typically produce organic carbon well in excess of their ecosystem requirements (net autotrophic), and it is estimated that a large proportion of the organic material (~ 40%) is exported to the surroundings as particulate and dissolved matter (Duarte and Cebrian 1996). Drift macrophytes constitute significant enrichment of organic C to the benthos and provide important spatial subsidies that support high levels of secondary production in adjacent communities (Vetter 1994; Harrold et al. 1998; Filbee-Dexter and Scheibling 2014), with episodic events such as high winds and storms facilitating massive C export fluxes (Dierssen et al. 2009). On a global scale, macroalgae have a large C sequestration capacity. Preliminary analyses estimate that around 173 Tg C yr^{-1} is sequestered, a value that exceeds C sequestration by angiosperm-based aquatic habitats (Krause-Jensen and Duarte 2016).

The important role of marine macroalgae for coastal productivity was realized more than four decades ago (Mann 1973). Despite this, productivity rates of macroalgal canopies and their role in the ocean C budget remains poorly quantified (Krause-Jensen and Duarte 2016; Duarte 2017). Performing detailed in situ studies on the production, degradation, and export potential of organic C within macroalgal canopies is challenging: traditional flux measurement techniques such as benthic chambers are difficult to apply to rocky outcrops

*Correspondence: karl.attard@biology.sdu.dk

and coarse sediment deposits, where these habitats often prevail (Glud et al. 2010). Additionally, chambers enclose only a small surface area of the canopy (~ 0.1 m^2), incubation times are short (~ 1 h) (Tait and Schiel 2010; Bordeyne et al. 2017), and the enclosure process excludes natural variations in hydrodynamics that may affect photosynthetic rates of the enclosed algae (Mass et al. 2010). Biomass addition techniques (e.g., Zieman 1974) have been applied extensively to study productivity rates of submerged vegetation. However, this method is time-consuming, destructive, underestimates true productivity rates, and cannot resolve short-term (hourly to daily) dynamics (Long et al. 2015*a*).

The aquatic eddy covariance (AEC) technique is a recent technological development that overcomes many of these issues. It quantifies benthic oxygen fluxes noninvasively, includes a large surface area of the seabed (tens of square meter) in its measurement and produces benthic fluxes for consecutive 15 min time periods over 24 h or more (Berg et al. 2003; Berg et al. 2007). From this, the daily net ecosystem metabolism (*NEM*), representing the integrated balance between habitat primary productivity versus respiration in a 24 h period, can be calculated either as the sum of daytime and nighttime fluxes weighted to the hours of day and night, respectively (Long et al. 2013; Attard et al. 2014), or as an integration of the AEC fluxes over 24 h (Hume et al. 2011; Rheuban et al. 2014*b*; Attard et al. 2015). Daily *NEM* O_2 fluxes can then be converted to C equivalents. Positive *NEM* values indicate a surplus of organic C production (net autotrophy), which results in accumulation of vegetation biomass within the habitat and/or export of particulate or dissolved matter to its surroundings. When the habitat is consuming more organic C than is being produced, *NEM* is negative. Therefore, by quantifying the *NEM* and the canopy standing biomass over time, it is possible to estimate the organic C export rate, which permits novel assessments on the role of macroalgal canopies within the marine C cycle.

Fucus vesiculosus (Linnaeus, 1753), commonly known as "bladder wrack," is a prominent species in temperate and Arctic coastal waters and it forms extensive canopies in the central Baltic Sea region (Råberg and Kautsky 2007). *F. vesiculosus* canopies occur most commonly at moderately exposed sites, with a maximum depth distribution limit located at ~ 6% of surface irradiance levels (Torn et al. 2006). Gas spaces on its fronds not only maintain canopy posture and facilitate spore dispersal but also accumulate considerable oxygen under illumination (Aleem 1969). Fucoid beds harbor greater macrofaunal abundance and biomass of small crustaceans than nonfucoid vegetated sites (Råberg and Kautsky 2007) and are important foraging grounds for commercially important fish such as perch (*Perca fluviatilis*) (Lappalainen et al. 2001). Despite the widespread occurrence of the species, *F. vesiculosus* canopies vary in their spatial extent and depth distribution in response to environmental drivers. In the Baltic Sea, canopies of *F. vesiculosus* have undergone large changes in extent and depth distribution (Kautsky et al. 1986; Torn et al. 2006). High nutrient loading of coastal waters has led to eutrophication and a decrease in sunlight transmittance, favoring instead proliferation of opportunistic ephemeral macroalgae such as the green alga *Ulva intestinalis* and the free-living brown alga *Pilayella littoralis*. In contrast, in the Arctic, the species is expected to expand to higher latitudes as the sea-ice cover diminishes (Krause-Jensen and Duarte 2014). The impacts this has had on the biodiversity of seafloor communities, including species' abundance, community structure, and living-mode of the benthos (mobility, feeding capabilities, and predator–prey interactions) are well documented (Bonsdorff 1992; Norkko and Bonsdorff 1996; Norkko et al. 2000; Råberg and Kautsky 2007). However, little is known about the effects these changes have had on seafloor primary productivity and the C cycle of the Baltic Sea and elsewhere.

The main objective of this study was to understand the role of perennial macroalgal canopies for primary productivity and organic C cycling dynamics in near-shore waters. We quantified rates of *F. vesiculosus* canopy *NEM* from benthic oxygen flux measurements using the AEC technique at a single location in the Baltic Sea multiple times within a year. The AEC measurements were complemented with biological surveys, which were performed in parallel with the AEC measurements to monitor *F. vesiculosus* canopy abundance and biomass. Based on regression analysis of the AEC fluxes and seabed sunlight availability (photosynthetically active radiation, [PAR]), we developed a simple predictive model for estimating daily canopy *NEM* continuously over 1 yr. This approach enabled us to evaluate canopy productivity on timescales ranging from 1 h to 1 yr, permitting for the first time detailed assessments of the productivity and potential rate of organic C export of a broadly distributed but understudied key coastal habitat.

Materials and methods

Study location and sampling

Seasonal sampling was performed on a macroalgal canopy situated close to the island archipelago of Spikarna (59°48.40N, 23°12.26E), located 4.4 km SW from the Tvärminne Zoological Station in SW Finland (Fig. 1A). This location is typical of the extensive Finnish rocky coastline and Archipelago Sea region. A submerged rocky outcrop at a water depth of 2 m was colonized by a continuous ~ 50 m × 50 m macroalgal bed consisting primarily of the canopy-forming brown alga *F. vesiculosus* (Fig. 1B, C). Benthic oxygen flux measurements and biological sampling of the *F. vesiculosus* canopy were carried out at this site on five occasions between August 2016 and June 2017 (August, October, and December 2016 and March and June 2017).

Benthic oxygen flux measurements

Benthic oxygen fluxes were quantified in situ using the AEC technique (Berg et al. 2003). Our AEC systems are very

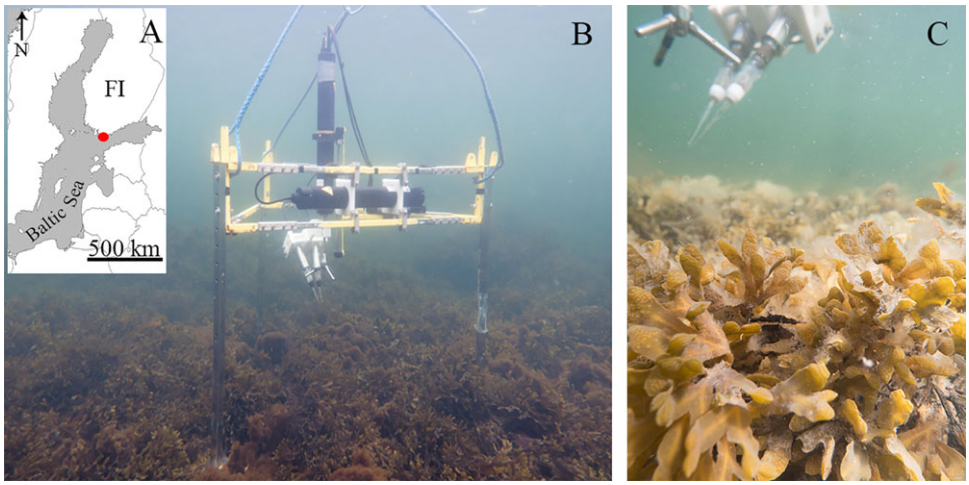

Fig. 1. **(A)** Location of our study site in Southwest Finland (red circle). **(B)** AEC instrumentation deployed at the site, and **(C)** a close-up of the *F. vesiculosus* canopy and the AEC sensors. Note that gas spaces (receptacles) are present on the apical tips. The height of the eddy covariance frame in (B) is 90 cm and the canopy height in (C) is ~ 20 cm. [Color figure can be viewed at wileyonlinelibrary.com]

similar to the original design used by Berg and Huettel (2008), consisting of fast-response oxygen microsensors (Clark-type, Revsbech [1989]; $T_{90} \leq 0.3$ s, low stirring sensitivity < 1%, Gundersen et al. [1998]) interfaced with a 6 MHz acoustic velocimeter (Nortek) via submersible amplifiers (McGinnis et al. 2011). Two oxygen microsensors were used simultaneously for redundancy and inter comparison purposes and were attached to the stem of the velocimeter using a polyoxymethylene mounting that allowed positioning the sensors at an angle of ~ 60° relative to the velocimeter, with the ~ 20 μm microsensor tips located 0.5 cm away from the instrument's 1.5 × 1.5 cm measurement volume (McGinnis et al. 2011). Instrumentation was mounted onto a sturdy aluminum tripod frame and was affixed to the frame so that the measurement volume was located ~ 35 cm above the seabed, well above the canopy height (Fig. 1B, C). A PAR sensor (LI-192, Li-Cor), a dissolved oxygen optode (Dissolved Oxygen Logger U26–001, HOBO), and a saltwater conductivity sensor (Salinity Data Logger U24–002-C, HOBO) located on the AEC frame logged transmitted (seabed) PAR, dissolved oxygen concentration, water temperature, and salinity at 5 min intervals throughout each deployment. AEC instrumentation was deployed by divers. The instrument was oriented within the predominant water flow direction (magnetic N-S), and care was taken to position the instrument level with the seafloor. Once deployed, the velocimeter measured the actual distance between the sensor measurement height and the seabed, before proceeding to log flow velocity and oxygen microsensor output in continuous sampling mode at 32 Hz. Individual deployments lasted 3–4 d.

Biological sampling

To relate the seasonal AEC measurements to the macroalgal canopy, abundance and biomass of *F. vesiculosus* were quantified seasonally, in conjunction with the AEC measurements at the end of each deployment. Biological sampling was performed by divers within an 80 m^2 circular area on the seafloor, with the AEC instrument located in its center. Eight 5 m-long weighted guidelines were used to delimit eight 45° direction sectors within the circle (Rodil et al. unpubl.). Abundance of *F. vesiculosus* (ind. m^{-2}) within this area was quantified by randomly placing quadrats (50 cm × 50 cm polyvinylchloride frames) within the eight direction sectors, and then enumerating the individuals in situ. For the *F. vesiculosus* standing biomass estimation, eight intact *F. vesiculosus* individuals, one from each direction sector, were sampled carefully using large mesh bags (0.5 mm mesh size). In the laboratory, *F. vesiculosus* individuals were oven dried to constant weight at 60°C and the dry weight was assessed to the nearest 0.1 g. Macroalgal dry weight was converted to organic C assuming a conversion ratio for Baltic Sea *F. vesiculosus* of 1.00 g dw: 0.35 g C (Ilvessalo and Tuomi 1989).

Oxygen flux extraction

Benthic oxygen fluxes were extracted from the measured 32 Hz velocity and oxygen microsensor data streams following established protocols for bin-averaging the measured 32 Hz data to 8 Hz, O_2 sensor calibration, detrending, and quality-checking individual flux intervals for anomalous data (Berg et al. 2003; Lorrai et al. 2010; Berg et al. 2013). Oxygen fluxes for consecutive 15 min intervals were extracted from the 8 Hz data using the software package EddyFlux version 3.00 (P. Berg, unpubl.). The eddy flux is calculated as $\overline{w'C'}$, where w' is the fluctuating vertical velocity around its mean, and C' is the fluctuating O_2 concentration around its mean, and the overbar symbolizes a time period average of 90 s that is sufficiently large to include the flux-contributing turbulent eddies

(Berg et al. 2003). Following careful analysis of mean oxygen concentration dynamics, which were easily distinguishable from shorter term turbulence-driven variations, w' and C' were isolated from a 90 s running mean (Berg et al. 2003; McGinnis et al. 2008; Berg et al. 2013). Individual 15 min fluxes were then evaluated for their quality by carefully screening the 8 Hz oxygen concentration and cumulative instantaneous flux $w'C'$ for anomalous variations. Large jumps or spikes in oxygen concentration, typically caused by particles colliding with the sensors, were excluded (Berg et al. 2013). Once quality checked, we assessed the sensitivity of the eddy fluxes to coordinate transformation and data shifting. Coordinate corrections typically are required for measurements in complex flow conditions or due to instrument leveling errors, to exclude horizontal flux projections into the vertical eddy flux (Reimers et al. 2012; Lorke et al. 2013). Sensor separation distances and stirring sensitivity effects (McGinnis et al. 2008; Donis et al. 2015; Holtappels et al. 2015) were evaluated as being of minor importance to the resolved fluxes (< 10%). The screened 15 min oxygen fluxes were subsequently bin-averaged to 1 h intervals (± SD; n = 4) for interpretation, with units of mmol m^{-2} h^{-1}. For multiple days of eddy flux data, the fluxes were bin-averaged by the hour of day. Daily *NEM* rates were determined in units of mmol m^{-2} d^{-1} by integrating the hourly fluxes over 24 h.

Eddy flux footprint characteristics

For each sampling campaign, the size and shape of the seafloor surface area included in the AEC flux measurements, the "flux footprint," was investigated from measurements of seafloor hydraulic roughness (z_0) and sensor measurement height, as described by Berg et al. (2007). The mean z_0 was computed from the flow velocity data streams using a multiple-step process. First, the complex Reynolds stress was calculated from streamwise (u), traverse (v), and vertical (w) velocity components, that were decomposed into a mean and a fluctuating velocity as $u = \overline{u} + u', v = \overline{v} + v'$, and $w = \overline{w} + w'$. From this, the friction velocity (u_*) was calculated as $u_*^2 = \overline{u'w'}^2 + \overline{v'w'}^2$ (Inoue et al. 2011). Subsequently, z_0 was calculated as $z_0 = z \times \exp\left(-\kappa \times \frac{U}{u_*}\right)$, where z is the AEC sensor measurement height above the seabed, κ is the Von Kármán constant (0.41), and U is the mean flow velocity magnitude (Wüest and Lorke 2003). The length, width, and region of maximum contribution (X_{max}) within the AEC flux footprint were calculated for each sampling campaign using the equations provided by Berg et al. (2007). The estimated length and width of the flux footprint area were used to estimate surface area by assuming that the footprint was elliptical in shape.

Annual estimate of canopy NEM

A regression analysis was performed to develop a predictive model for estimating canopy daily *NEM* continuously over 1 yr. First, daily *NEM* for the five measurement campaigns was related to the corresponding seabed PAR (daily integrated; mol PAR m^{-2} d^{-1}) using nonlinear regression and the asymptotic exponential function $NEM = a - b \times c \hat{} PAR$. The fitting function was then applied to year-round measurements of seabed PAR. Year-round PAR at the *F. vesiculosus* canopy was estimated from measurements of incoming PAR (SMEAR III Station, University of Helsinki) that were corrected for attenuation, by applying attenuation factors that were determined in situ for different seasons during each measurement campaign. Daily canopy *NEM* was integrated over the year to compute annual canopy *NEM* in mol O_2 m^{-2} yr^{-1} and in kg C m^{-2} yr^{-1} (assuming respiratory and photosynthetic O_2 : CO_2 of 1.0). This approach is similar to the one used in the studies by Rheuban et al. (2014*a*) and Attard et al. (2015) to quantify annual *NEM* in seagrass beds and coralline algal beds.

Oxygen storage within *F. vesiculosus* gas spaces

We explored whether gas storage within intercellular air spaces of *F. vesiculosus* could be significant. Earlier studies have documented considerable oxygen accumulation within macroalgal gas spaces under illumination (Damant 1936; Vallance and Coult 1951; Tammes 1954; Aleem 1969). To investigate this potential mechanism, oxygen microsensors (fiber-optode, 300 μm tip diameter, T_{90} < 10 s) connected to an optical oxygen meter (FireStingO_2 4-channel, PyroScience) were inserted into gas spaces of intact *F. vesiculosus* plants that were collected from the study area in June, and percentage air saturation was logged within the bladders at 5 s intervals while exposing the submerged plant to light–dark cycles in temperature-controlled (10°C) laboratory flow-through aquaria, under ~ 100% air saturated water. A light-emitting diode panel that accurately simulates natural outdoor light was used for illumination (~ 400 μmol PAR m^{-2} s^{-1}), and a dissolved oxygen optode (Dissolved Oxygen Logger U26–001, HOBO) logged dissolved oxygen concentration in the aquarium water at 5 min intervals.

Results

Environmental conditions

The environmental conditions for the five measurement campaigns are summarized in Table 1. Water temperature ranged from 1.3 ± 0.3°C in March to 15.9 ± 0.6°C in August (mean ± SD). Salinity was between 5.6 ± 0.0 and 6.4 ± 0.1 throughout the year (mean ± SD). Daily dissolved oxygen concentration was highest in March (435 ± 21 μmol L^{-1}) and lowest in August (277 ± 26 μmol L^{-1}) (mean ± SD). Oxygen saturation ranged from 90% ± 2% in December to 103% ± 5% in March (mean ± SD). Diel variations in dissolved oxygen concentration were evident in all seasons. The highest diel amplitudes were observed in June (120 μmol L^{-1}) and August (111 μmol L^{-1}), with intermediate values observed in March (63 μmol L^{-1}) and October (56 μmol L^{-1}), and the lowest values in December (16 μmol L^{-1}). Daily integrated

Table 1. Environmental conditions (mean ± SD) and eddy covariance dataset duration for the five measurement campaigns. Flow velocity is measured by the velocimeter 30 cm above the canopy.

Sampling campaign start date	Dataset duration (h)	Water temperature (°C)	Mean flow velocity (cm s^{-1})	Salinity	Mean oxygen concentration (μmol L^{-1})	Mean air saturation (%)	Daily integrated seabed PAR (mol m^{-2} d^{-1})
24 Aug 2016	55	15.9 ± 0.6	3.4 ± 2.5	5.7 ± 0.0	277 ± 26	92 ± 9	18.6
13 Oct 2016	31	9.3 ± 0.8	2.2 ± 0.9	5.9 ± 0.0	318 ± 14	92 ± 4	3.1
01 Dec 2016	72	3.4 ± 0.5	2.8 ± 3.1	5.6 ± 0.0	361 ± 7	90 ± 2	1.0
23 Mar 2017	65	1.3 ± 0.3	4.8 ± 2.7	6.4 ± 0.1	435 ± 21	103 ± 5	5.4
06 Jun 2017	67	9.6 ± 0.5	1.7 ± 2.0	5.7 ± 0.0	342 ± 30	99 ± 9	30.7

seafloor PAR varied by approximately 30-fold, from 30.7 mol m^{-2} d^{-1} in June to 1.0 mol m^{-2} d^{-1} in December.

Seasonal canopy dynamics

Our seasonal measurements of *F. vesiculosus* abundance indicate that the number of canopy-forming individuals remained more or less constant throughout the year, ranging from 15 ± 4 ind. m^{-2} in October to 19.5 ± 3 ind. m^{-2} in August (mean ± SD, n = 8), with no significant differences observed between the five measurement campaigns (one-way ANOVA $F_{5,42}$ = 1.22; p = 0.32; Fig. 2). However, the canopy standing biomass and the estimated C standing stock decreased significantly from summer to late winter (from 0.4 ± 0.2 kg C m^{-2} in August to 0.2 ± 0.1 kg C m^{-2} in March; one-way ANOVA $F_{5,42}$ = 3.47; p = 0.01), and then amassed biomass to values comparable to the previous summer between March and June (0.4 ± 0.2 kg C m^{-2}; Fig. 2). Length of *F. vesiculosus* individuals (mean ± SD, n = 8) ranged from 33 ± 6 cm in December to 40 ± 6 cm in August, and the canopy height was typically 15–20 cm.

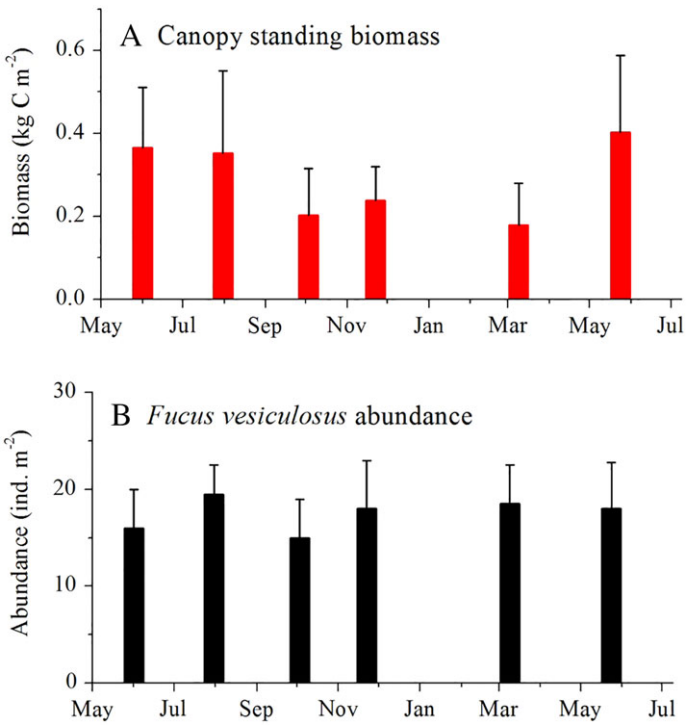

Eddy fluxes: Hourly dynamics

Each measurement campaign yielded 1–3 d of continuous, high-quality eddy flux data. The hourly fluxes document considerable temporal dynamics in response to changing environmental conditions such as PAR over diel periods (Fig. 3). High flow velocities of up to 10.8 cm s^{-1} at this moderately exposed site combined with a rough seabed surface maintained well-developed turbulent conditions throughout the selected datasets (Fig. 3). Linear cumulative instantaneous fluxes evidenced a favorable turbulent flux signal for extracting eddy fluxes (Fig. 3C). The mean ± SD hydraulic roughness (z_0) ranged from 2.1 ± 1.3 cm (n = 322) in June to 3.6 ± 1.3 cm (n = 193) in December, corresponding to a flux footprint length (area) range between 26 m (35 m^2) and 42 m (56 m^2) (Berg et al. 2007). The global average footprint length for the five measurement campaigns was 30 ± 7 m (n = 5) and the average area was 40 ± 9 m^2 (n = 5). The region of maximum flux contribution (X_{max}) within the footprint area was located between 0.6 and 1.5 m upstream from the instrument (global average = 0.8 ± 0.4 m; n = 5).

The hourly eddy fluxes were broadly correlated with the PAR availability in all seasons, where sunlight reaching the canopy stimulated a measurable photosynthetic oxygen production (Fig. 4A, B). The highest hourly net oxygen release rates by the *F. vesiculosus* canopy were observed in August. Here, canopy PAR of up to ~ 900 μmol quanta m^{-2} s^{-1} corresponded to net oxygen release rates by the canopy of up to 35.2 ± 9.1 mmol m^{-2} h^{-1}. As measurements progressed into the autumn, the amount of available sunlight at the canopy surface decreased to a maximum of ~ 150 μmol PAR m^{-2} s^{-1}, with a corresponding decrease in the maximum observed net oxygen release rates (4.6 ± 0.3 mmol m^{-2} h^{-1}). Canopy PAR and oxygen release rates were lowest in early winter (December). During this measurement campaign, a maximum of ~ 90 μmol PAR m^{-2} s^{-1} was measured at the canopy surface,

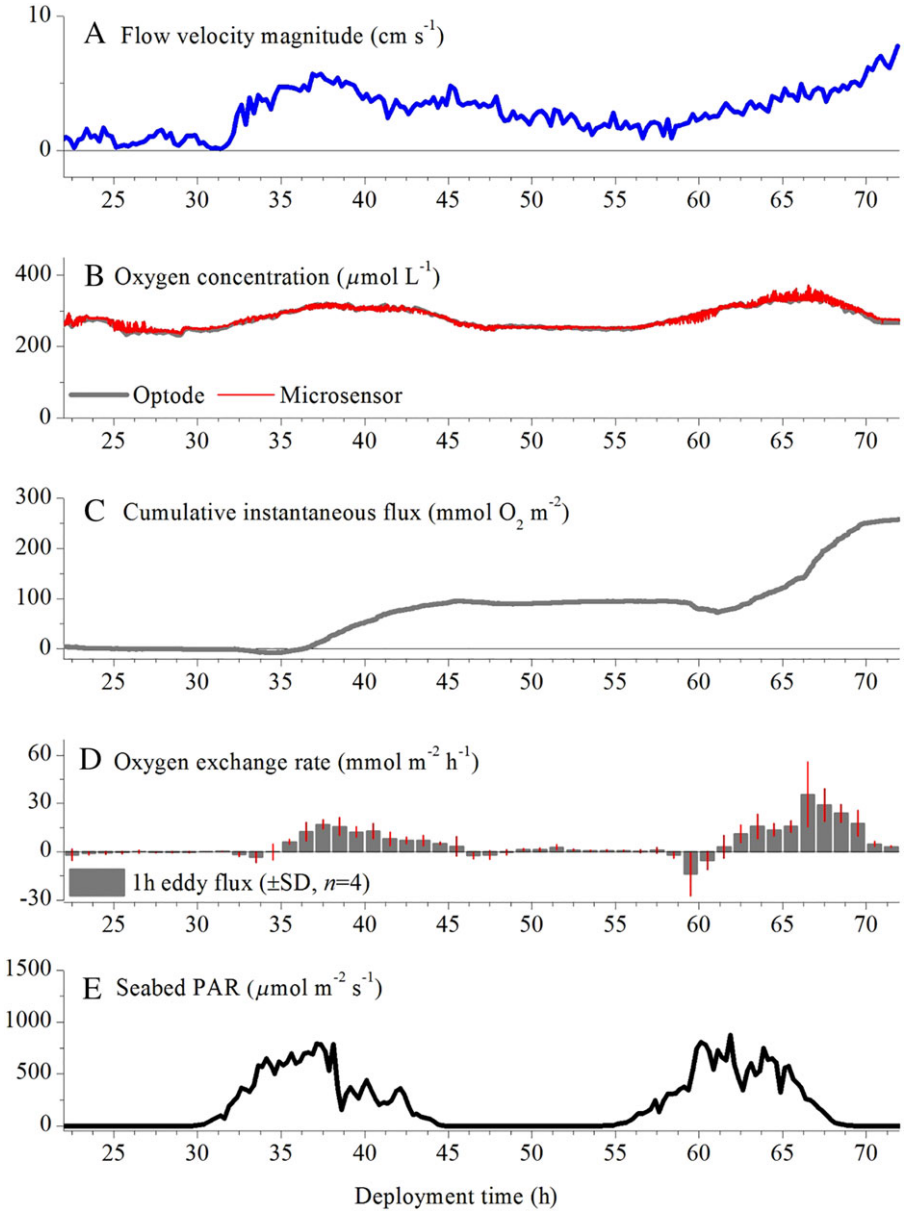

and daytime oxygen fluxes were less negative than nighttime values, but were low in magnitude compared to daytime fluxes measured during the other campaigns (up to 0.2 ± 0.2 mmol m^{-2} h^{-1}). As sunlight intensity and the duration of the photic period increased toward the end of winter, remarkably high hourly rates of net oxygen production were measured, despite the cold water temperatures. In March, oxygen fluxes reaching 16.7 ± 5.2 mmol m^{-2} h^{-1} were measured under maximum PAR of ~ 250 μmol m^{-2} s^{-1} and water temperatures of just 1.3 ± 0.3°C. High canopy net oxygen release rates of up to 23.4 ± 7.7 mmol m^{-2} h^{-1} were maintained through to early summer (June), under the highest measured canopy PAR values for our seasonal measurement campaign of up to ~ 1350 μmol PAR m^{-2} s^{-1} (Fig. 4).

The eddy flux datasets for June, August, and October showed interesting hourly dynamics where high oxygen release rates were maintained through to the end of the day under very low light levels (e.g., 3.6 ± 1.1 mmol m^{-2} h^{-1} under ~ 4 μmol PAR m^{-2} s^{-1} in June; Fig. 4). Furthermore, dark rates of oxygen uptake during these months overall were very low. During some nighttime periods with well-developed turbulent conditions in June and in August, nighttime fluxes were around 0 mmol m^{-2} h^{-1} or were even positive, suggesting minimal oxygen uptake or even an apparent oxygen

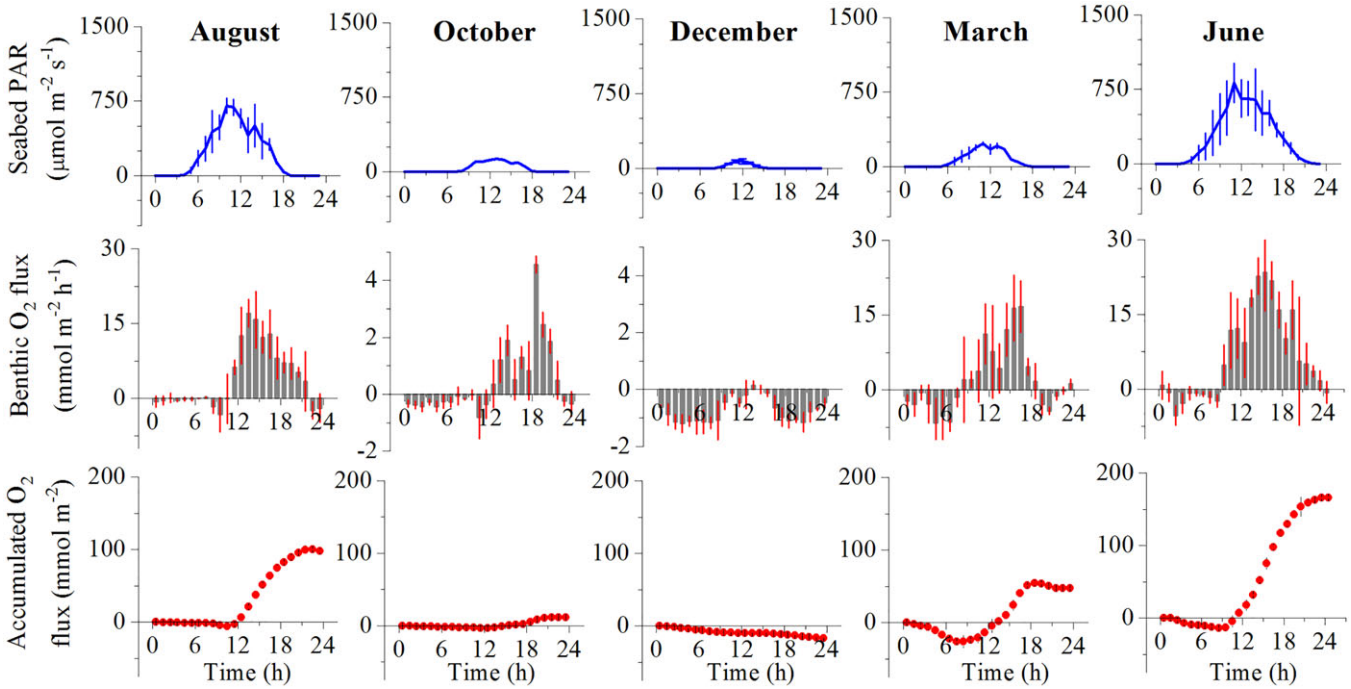

release by the canopy under dark conditions (Figs. 3–4). This repeated pattern could not be explained by accounting for uncertainties in eddy flux extraction, namely from (a) changes in water flow velocity and oxygen concentration (Holtappels et al. 2013; Rheuban et al. 2014*b*), (b) accumulation/depletion dynamics of oxygen within the canopy (Hendriks et al. 2014; Long et al. 2015*b*), (c) changes in water flow direction, (d) flux sensitivity to instrument coordinate rotation (Reimers et al. 2012; Lorke et al. 2013), and (e) response time of the AEC sensors to changes occurring at the seafloor surface (integration time; Rheuban and Berg 2013). The original fluxes therefore were of high quality and were representative of the true benthic flux. Subsequently, we considered whether gas storage within gas spaces of *F. vesiculosus* could be significant. Intact specimens of *F. vesiculosus* that were collected from the field in the morning had high oxygen saturation levels within their gas spaces (~ 33% oxygen), and this value increased to ~ 40% following 18 h of illumination (Fig. 5). Oxygen content decreased exponentially with time in the dark, but remained above air saturation levels of the ambient water for ~ 12 h, much longer than the typical nighttime duration for this time of the year (June, ~ 5 h). Despite there being lower light levels in the experimental setup relative to typical summer time field conditions (400 μmol PAR m^{-2} s^{-1} vs. ~ 1200 μmol PAR m^{-2} s^{-1}), these results indicate that there is considerable oxygen accumulation and drawdown from within *F. vesiculosus* gas spaces during day and night periods, respectively. Furthermore, there exists a disequilibrium between internal (gas space) and external (water phase) oxygen concentration, and interestingly, this concentration gradient indicates a potential for oxygen release by the canopy under dark conditions, which is consistent with the dynamics we observed in the eddy covariance fluxes. Quantifying photosynthetic production and respiration rates of gas-storing macroalgae from in situ hourly fluxes or from external changes in oxygen concentration (using, e.g., eddy covariance, chamber incubations, or from microprofiling measurements within boundary layers above fronds) would thus underestimate the true gross metabolic activity. In our study, however, we focus on the daily *NEM*, which is calculated from continuous flux time series lasting one or more days. This approach would cancel out the gas storage effect and would provide robust daily rate estimates of *NEM*.

Eddy fluxes: Daily and seasonal canopy productivity

Oxygen production by the *F. vesiculosus* canopy exceeded oxygen consumption over 24 h in four out of the five measurement campaigns (Fig. 4C). Daily *NEM*, quantified as the integration of continuous hourly eddy fluxes over 24 h, indicated that the canopy was strongly net autotrophic in summer (June = 166 mmol O_2 m^{-2} d^{-1} and August- = 98 mmol O_2 m^{-2} d^{-1}). Net autotrophy persisted in autumn (October = 11 mmol O_2 m^{-2} d^{-1}) and in late winter (March = 48 mmol O_2 m^{-2} d^{-1}), but the canopy was net heterotrophic in early winter (December = –17 mmol O_2 m^{-2} d^{-1}; Fig. 4C).

Following a regression analysis of daily canopy *NEM* and light (PAR) availability, we found that the daily *NEM* for the five measurement campaigns was highly correlated with the

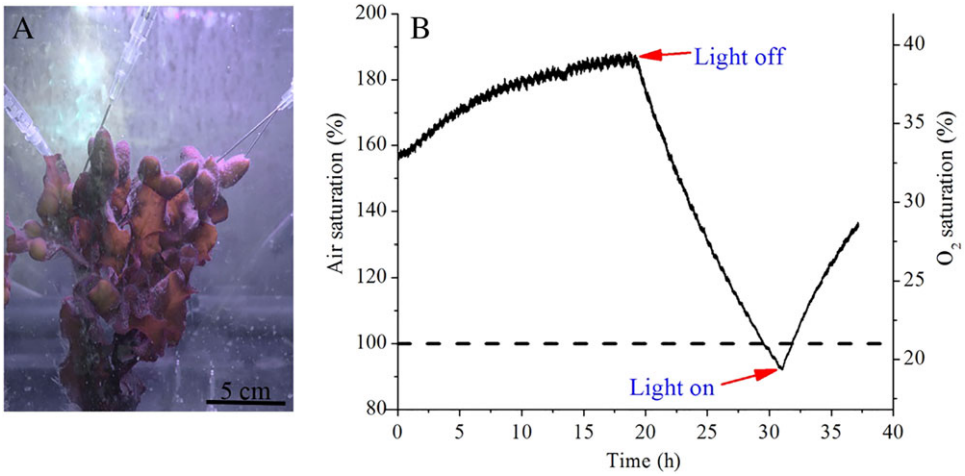

corresponding daily integrated PAR reaching the *F. vesiculosus* canopy surface. The asymptotic exponential function $NEM = a - b \times c \hat{} PAR$ gave a remarkably good fit ($R^2 = 0.99$) to the measured data, providing us with a simple empirical relationship for estimating canopy *NEM* (Fig. 6). PAR attenuation factors for the different seasons were derived by relating the measurements of incoming PAR vs. canopy PAR using linear regression. The R^2 value was 0.84 in March, 0.92 in December, 0.94 in August, 0.95 in June, and 0.96 in October. Applying the established fitting function to year-round canopy PAR (Fig. 7A) yielded continuous daily *NEM* throughout the 12 months of our measurement period (Fig. 7C). The predictive model was based on canopy PAR that ranged from 0.1 mol photons m^{-2} d^{-1} (model *NEM* = –28 mmol O_2 m^{-2} d^{-1}) in December to 39.6 photons mol m^{-2} d^{-1} (model *NEM* = 183 mmol O_2 m^{-2} d^{-1}) in June (Fig. 7A, C). This variability range was similar to the range observed in the field during our five measurement campaigns. Here, daily integrated canopy PAR ranged from 1.0 mol m^{-2} d^{-1} in December (measured *NEM* = –17 mmol O_2 m^{-2} d^{-1}) to 30.7 mol m^{-2} d^{-1} in June (measured *NEM* = 166 mmol O_2 m^{-2} d^{-1}; Table 1; Fig. 4), indicating that our measurements covered a large part of the seasonal variability in daily PAR that the *F. vesiculosus* canopy was exposed to in situ. The results from this simple dynamic modeling exercise based on the empirical relationship that we established between daily PAR and *NEM* indicate that the canopy was net autotrophic (*NEM* > 0 mmol O_2 m^{-2} d^{-1}) for 246 d yr^{-1}, with high net autotrophy (*NEM* > 100 mmol O_2 m^{-2} d^{-1}) observed during 150 d yr^{-1}. The canopy was net heterotrophic (*NEM* < 0 mmol O_2 m^{-2} d^{-1}) from mid-November to mid-February, equivalent to 33% (or 119 d) of the year (Fig. 7C). Integrating daily *NEM* over the year indicated that the *F. vesiculosus* canopy was highly net autotrophic on an annual basis, with annual canopy *NEM* amounting to 25.2 mol O_2 m^{-2} yr^{-1} or 0.3 kg C m^{-2} yr^{-1} (Fig. 7D).

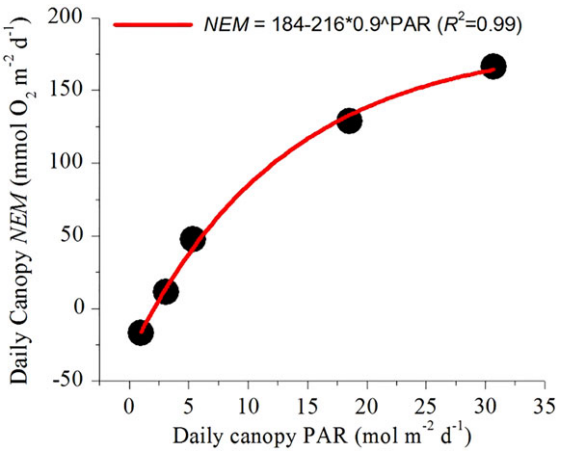

Fig. 6. Relationship between daily canopy *NEM* and seabed light (PAR, daily integrated). [Color figure can be viewed at wileyonlinelibrary.com]

Discussion

Hourly, daily, and seasonal canopy productivity

Our in situ AEC measurements integrating ~ 40 m^2 of seabed surface area document considerable oxygen production by the *F. vesiculosus* canopy year-round, with hourly net production rates of up to 35 ± 9 mmol m^{-2} h^{-1} in late summer under maximum water temperature of ~ 16°C and canopy PAR of up to ~ 900 μmol quanta m^{-2} s^{-1}. Even though it is likely that the hourly rates underestimate the true net production due to gas storage, the rate magnitudes are still high, and are comparable to rates observed in shallower, dense seagrass canopies at lower latitude exposed to higher PAR and warmer water temperature (Rheuban et al. 2014*b*). Macroalgal canopies in other geographical locations similarly express remarkably high hourly rates of productivity in excess of 100 mmol C m^{-2} h^{-1} during peak irradiance in summer (Tait and Schiel 2010; Bordeyne et al. 2017). Interestingly, high hourly rates of net

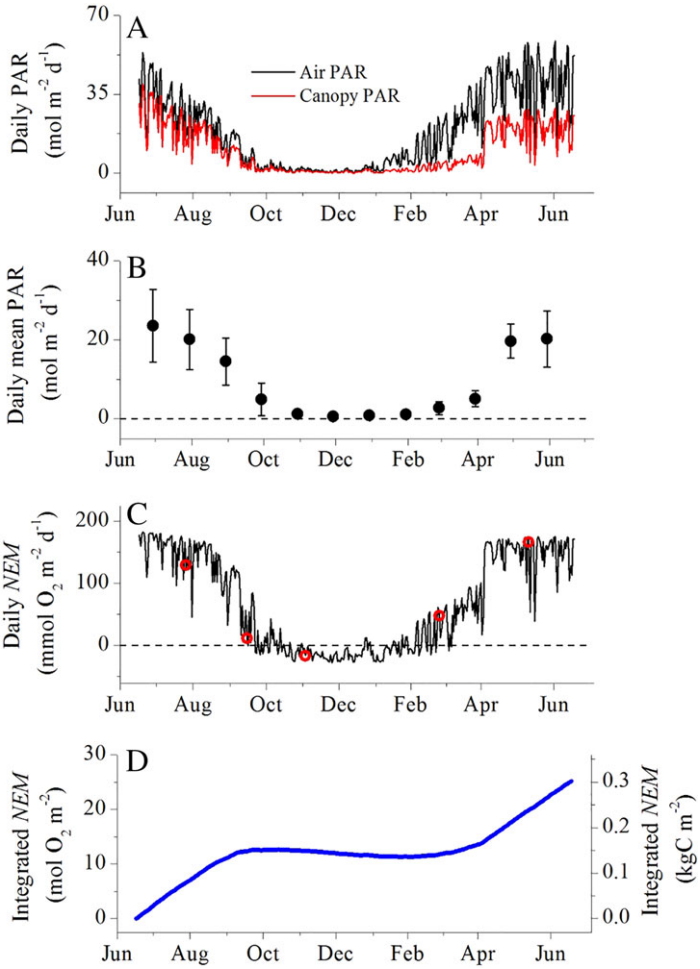

Fig. 7. Results from the predictive model showing **(A)** daily incoming PAR and transmitted (canopy) PAR, **(B)** mean daily canopy PAR for the 12 months (± SD), **(C)** modeled daily *NEM*, including measured values

oxygen production by the *F. vesiculosus* canopy > 15 mmol O_2 m^{-2} h^{-1} were not limited to the summer months but were also observed in late winter (March) under maximum PAR of ~ 250 μmol m^{-2} s^{-1} and water temperatures of just 1.3 ± 0.3°C. It is interesting to note that our seasonal measurements indicate key differences in the biogeochemical functioning of the canopy between early and late winter. In December, under water temperatures of 3.4 ± 0.5°C and daily PAR of 1.0 mol m^{-2} d^{-1}, a distinct light-response was evident in the eddy fluxes (Fig. 4), but respiration exceeded primary production over 24 h, and the canopy was net heterotrophic (*NEM* = –17 mmol m^{-2} d^{-1}). By contrast, in March, under colder water temperatures (1.3 ± 0.3°C) but higher light availability (5.4 mol m^{-2} d^{-1}) and a longer photic period, the canopy was net autotrophic (*NEM* = 48 mmol m^{-2} d^{-1}). These observations challenge traditional views on high-latitude seafloor ecosystems as being generally unproductive in winter with sluggish rates of activity. While early winter measurements indicate a net heterotrophic habitat relying on external or stored organic material to sustain ~ 75% of the daily C demand, our subsequent winter measurements performed in March indicate that macroalgal canopies are able to efficiently harvest the available light and are able to assimilate large amounts of C, more than is required to sustain the daily respiratory requirements of the canopy habitat. Indeed, positive daily *NEM* was observed in four of the five measurement campaigns. Comparison of these results to *NEM* estimates for other habitats worldwide (seagrass, macroalgae, coralline algal beds, bare sediments; considering only studies that computed the daily *NEM* from continuous diel measurements over 24 h) suggests that macroalgal canopies overall have amongst the highest (i.e., most positive) daily *NEM* (Fig. 8). While some studies have investigated productivity rates of *F. vesiculosus* in the Baltic Sea (Kairesalo and Leskinen 1986; Leskinen et al. 1992), studies on whole-canopy productivity remain few. Our results indicate that macroalgal canopies effect amongst the highest hourly rates of seafloor primary productivity, and are amongst the most highly net autotrophic habitats. The seasonal and annual *NEM* values we obtained in our study are high when compared to existing values for the pelagic environment nearby our study site. Annual phytoplankton gross productivity rates (depth-integrated over the ~ 10 m photic zone) quantified using ^{14}C incubations range from 74–170 g C m^{-2} yr^{-1}, with about two-thirds of phytoplankton productivity being respired within the water column (Kuparinen et al. 1984; Lignell et al. 1993). These results document the importance of seafloor primary production on an ecosystem level. The spatial extent and distribution of macroalgal canopies on the seafloor is likely to be an important factor in determining organic C assimilation, CO_2 drawdown and O_2 production rates in coastal waters.

Our laboratory measurements documented substantial oxygen accumulation and light-dependent dynamics within gas spaces of *F. vesiculosus*. Two types of intercellular gas spaces were identified on the thallus branches of the *F. vesiculosus* canopy we investigated: vesicles were located along the fronds at regular intervals on either side of the midrib, and receptacles were present at the apical tips. Earlier studies have documented considerable oxygen accumulation in macroalgae gas spaces under illumination (Damant 1936; Vallance and Coult 1951; Tammes 1954; Aleem 1969). Even though the gas space volume typically is small relative to that of the surrounding water, the accommodation coefficient of oxygen is ~ 40 times higher in air than in water. The degree of storage (E, in %) can be assessed on the basis of gas-to-water ratio and solubility of oxygen according to the equation: $E = p/\alpha(V_g \times 1000/V_f)$, where p is the fractional volume of oxygen in air (0.21), α is oxygen solubility in water, V_g is the gas volume, and V_f is the volume of incubated water (Sorrell and Dromgoole 1986). This equation implies that under conditions of instantaneous oxygen equilibrium between gas space and water, a 1% gas volume contains ~ 25% of all oxygen, and thus considerable oxygen storage potential. We propose that high oxygen

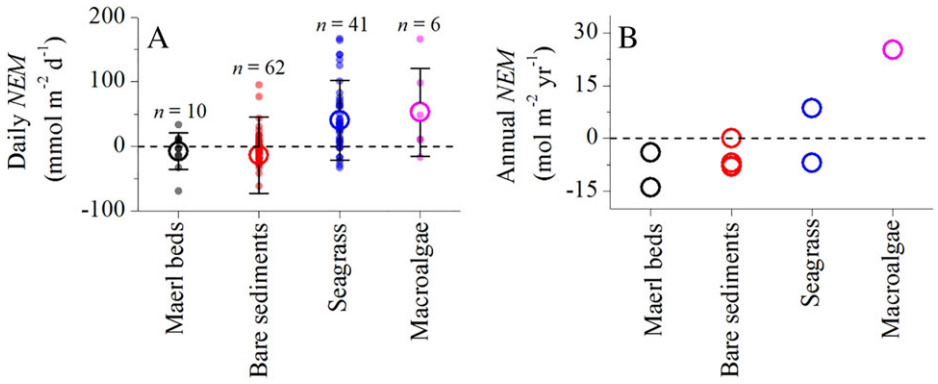

Fig. 8. Community *NEM* rates of various seafloor habitats worldwide on **(A)** daily and **(B)** annual timescales. Daily *NEM* (a) mean ± SD (large open symbols) and number of observations (*n*) for datasets that compute the daily *NEM* from continuous diel measurements over 24 h (Maerl beds: Attard et al. [2015], Martin et al. [2007], and Martin et al. [2005]; bare sediments: Attard et al. [2014], Attard et al. [2015], Berg et al. [2013], Chipman et al. [2016], Hume et al. [2011], Rheuban et al. [2014*a*], and Walpersdorf et al. [2017]; macroalgae: Gruber et al. [2017] and this study; Seagrass: Ganguly et al. [2017], Gruber et al. [2017], Hume et al. [2011], Lee et al. [2017], Long et al. [2015*b*], Moriarty et al. [1990], Olivé et al. [2016], Pollard and Moriarty [1991], and Rheuban et al. [2014*b*]). Annual data (B) are from studies that consider daily and seasonal *NEM* when computing the annual estimate (Maerl beds: Attard et al. [2015] and Martin et al. [2007]; bare sediments: Attard et al. [2015], Chipman et al. [2016], and Rheuban et al. [2014*a*]; Seagrass: Rheuban et al. [2014*a*]; Macroalgae: this study). [Color figure can be viewed at wileyonlinelibrary.com]

release rates by the seabed at the end of the day, as well as low oxygen consumption at night, as we observed in our AEC datasets during periods with high metabolic activity, are consistent with the gas storage effect. Oxygen accumulation in gas spaces during the day would buffer oxygen consumption requirements at night, thereby reducing the drawdown requirements of oxygen from the water column. These observations contrast with seafloor oxygen flux dynamics observed in other habitats such as seagrass beds and bare sediments, which typically show higher seafloor oxygen uptake rates in the evening than in the morning due to photosynthesis-coupled respiration (Fenchel and Glud 2000; Rheuban et al. 2014*b*). Further measurements are required to constrain the effects of oxygen storage on the oxygen budget within macroalgal canopies, in order to better understand its ecological and biogeochemical significance.

Annual canopy NEM

The results from the predictive model indicate that daily *NEM* was positive for 246 d (or two-thirds) of the year (Fig. 7B). When integrated over the year, the *F. vesiculosus* canopy was highly net autotrophic, with annual *NEM* amounting to ~ 25 mol O_2 m^{-2} yr^{-1} (~ 0.3 kg C m^{-2} yr^{-1}; Fig. 7C). The process of deriving annual *NEM* based on the empirical relationship between daily integrated PAR and *NEM* for the five measurement campaigns (Figs. 6–7) is a first-order approach that invokes several assumptions about the functioning of the canopy. In particular, this approach assumes that the daily balance between primary productivity and respiration over the course of the year is driven only by changes in the amount of daily irradiance reaching the seafloor, thus not directly accounting for other potentially important factors such as seasonal changes in standing biomass and community composition, sedimentation dynamics, light acclimation, and temperature effects. We estimated annual *NEM* using a second approach that is independent of the PAR-NEM relationship. In this second approach, the daily NEM values from the individual measurement campaigns were plotted over the year, and a Gaussian function was fitted to this data using a least-squares approach to interpolate between data points (OriginPro 8.5, OriginLab). The Gaussian function thus described daily NEM dynamics over 12 months, and the integrated value of this curve then represents the annual NEM. The fitting function gave a tight fit to the measured data (R^2 = 0.99), and the estimated annual *NEM* of 23.5 mol O_2 m^{-2} yr^{-1} was within 6% of our previous estimate (25 mol O_2 m^{-2} yr^{-1}). We can further constrain the minimum annual *NEM* and C export using the seasonal *F. vesiculosus* standing biomass measurements (Fig. 2). The decrease between summer and late winter (17 mol O_2 m^{-2} yr^{-1} [0.2 ± 0.2 kg C m^{-2}]), and the subsequent increase between winter and summer (17 mol O_2 m^{-2} yr^{-1} [0.2 ± 0.2 kg C m^{-2}]), represent the minimum annual rates of C export and *NEM*.

Very few studies have considered seasonal changes in canopy productivity on a community-scale when computing the annual estimate. To our knowledge, there exist none for macroalgal canopies. Comparison to available datasets for other habitats indicates that the annual *NEM* for the *F. vesiculosus* canopy is high. Martin et al. (2007) and Attard et al. (2015) found that coralline algal beds were net heterotrophic on an annual basis (–14 and –4 mol m^{-2} yr^{-1}, respectively), as were the bare sediments in the studies by Attard et al. (2015) (–7 mol m^{-2} yr^{-1}) and Rheuban et al. (2014*a*) (–8 mol m^{-2} yr^{-1}). Annual *NEM* of seagrass beds in the Virginia Coastal Reserve, ranged from net heterotrophic (–7 mol m^{-2} yr^{-1}) to net autotrophic (9 mol m^{-2} yr^{-1}) (Rheuban et al. 2014*a*). The *F. vesiculosus* canopy investigated in this study thus has higher annual *NEM* than some of the most productive seagrass beds (Fig. 8B), an observation that is in line

with the global synthesis on annual *NEM* of submerged vegetated habitats (Duarte 2017). The annual canopy *NEM* of 25 mol O_2 m^{-2} yr^{-1}, or 0.3 kgC m^{-2} yr^{-1}, is comparable to the global average estimate for macroalgal bed *NEM* of 0.4 kg C m^{-2} yr^{-1} (Krause-Jensen and Duarte 2016).

It is likely that the high daily and annual *NEM* rates associated with macroalgal canopies are a result of a combination of factors relating to high macroalgal primary productivity, low sediment accumulation rates within-habitat, and low herbivory rates. Macroalgal canopies typically colonize submerged rocky outcrops, having low sediment and detritus accumulation. Canopy-forming macroalgae such as *F. vesiculosus* have a high proportion of their biomass that is photosynthetically active when compared to other canopy-forming vegetation (e.g., seagrass), and thus are able to photosynthesize efficiently under low light and can assign a large proportion of their new production to growth (Markager and Sand-Jensen 1992). Production of anti-grazing compounds (Rohde et al. 2004) and high frond C : N (e.g., C : N of *F. vesiculosus* in the Baltic Sea ranges seasonally from ~ 15 to ~ 60, with an annual average of ~ 37) (Ilvessalo and Tuomi 1989) may restrict extensive canopy grazing. Furthermore, many marine invertebrates that are commonly associated with macroalgal canopies in the Baltic Sea, such as the isopod *Idotea balthica* and the bivalve *Mytilus edulis*, apparently lack the carbohydrases that are required to break down the plant tissue, and thus are not able to digest the plant material (Hylleberg Kristensen 1972). Altogether, these processes would favor low rates of community respiration within macroalgal canopies, with potential important implications for biogeochemical cycles and habitat functioning.

C export potential

Globally, it is estimated that a large proportion of macroalgal *NEM* (> 40%) is exported to surrounding environments (Duarte and Cebrian 1996; Krumhansl and Scheibling 2012; Krause-Jensen and Duarte 2016). Our measurements of *F. vesiculosus* abundance indicate that the number of canopy-forming individuals remained more or less constant throughout the year, with no significant differences observed between the five measurement campaigns (Fig. 2). However, the canopy standing biomass and the estimated C standing stock decreased significantly from summer to late winter (from 0.4 ± 0.2 kg C m^{-2} in August to 0.2 ± 0.1 kg C m^{-2} in March), and then amassed biomass to values comparable to the previous summer between March and June (0.4 ± 0.2 kg C m^{-2}). These measurements, in combination with our personal observations whilst surveying the canopy, indicate that a sizable canopy is present year-round. In addition to being a perennial habitat-forming structure, the canopy is a substantial source of organic matter to its surroundings. In our study, annual integrated values of canopy *NEM* indicate a surplus of organic C production amounting to 25 mol O_2 m^{-2} yr^{-1} (or 0.3 kg C m^{-2} yr^{-1}; Fig. 7D). When considering that there was no detectable accumulation of canopy biomass on an annual basis, nor a substantial accumulation of detritus on the rocky substratum within the macroalgal bed, we can assume that most of the surplus C produced by the canopy was exported as particulate and dissolved matter. Thus, our measurements indicate that annual net C export rates are comparable to the canopy standing biomass observed in summer. Due to the rocky nature of the underlying substrate, C burial within the habitat itself will be very low, so exchange of detritus will occur beyond the perimeter of the habitat itself (Krumhansl and Scheibling 2012). On multiple occasions in summer and in autumn, we observed vast underwater fields of unattached macroalgal detritus on the seabed of an enclosed embayment nearby the study site that consisted primarily of *F. vesiculosus* (Fig. 9). Factors such as seasonal decay, epiphyte growth, and grazing accelerate blade erosion and fragmentation (Knight and Parke 1950; Russell 1985; Krumhansl and Scheibling 2012; Anderson and Martone 2014). Additionally, physical forcing such as intensified wave energy and currents during storms, as well as seasonal ice scouring, would dislodge whole fronds and thalli, and thus would facilitate C export (Kiirikki and Ruuskanen 1996; Krumhansl and Scheibling 2012). Analysis of wind speed and direction data collected from a weather station nearby our sampling site (Hanko Russarö, Finnish Meteorological Institute) indicates a prevalence of southerly winds (wind directions > 90° and < 270°) from September to December, with high southerly winds (wind speeds > 10 m s^{-1}) being a common occurrence in October and November (data not shown). This period coincides with a substantial reduction in biomass in the *F. vesiculosus* canopy (Fig. 2), potentially indicating that these months are particularly important for particulate C export. Accumulations of drifting detritus constitute nourishment and a temporary habitat structure for opportunistic mobile taxa such as Ostracod crustaceans and the water snail *Hydrobia* spp. (Norkko et al. 2000). Conversely, given high enough abundance,

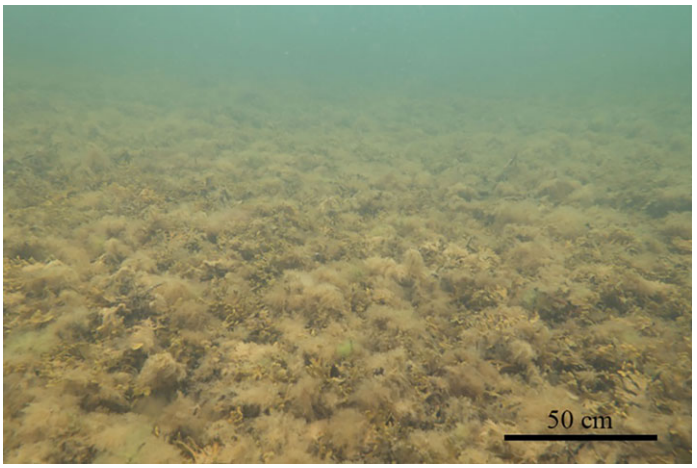

Fig. 9. Large underwater fields of unattached macroalgal detritus composed primarily of *F. vesiculosus* were observed in an enclosed embayment

drifting macroalgae can represent hotspots of anoxia and hydrogen sulfide production, generating adverse conditions to coastal biota and inducing large-scale mortality of sedentary macrobenthic populations (Norkko and Bonsdorff 1996; Glud et al. 2004; Norkko et al. 2013). The exported detritus is therefore an important spatial subsidy and a form of habitat connectivity within the coastal zone that can have positive as well as deleterious effects on aquatic ecosystems (Polis et al. 1997).

A proportion of the exported C by the canopy will be in dissolved form. Canopy-forming algae such as *F. vesiculosus* as well as other canopy-associated algae exude a proportion of their daily C fixation as dissolved organic carbon (DOC), which exchange with the surrounding water and could make up a significant proportion of the total DOC pool in coastal waters (~ 20%) (Wada and Hama 2013). Exudation rates for *F. vesiculosus* range from < 5% to 40% of net C production and vary seasonally (Sieburth 1969; Carlson and Carlson 1984), with global average values for macroalgae DOC exudation at ~ 20% of *NEM* (Maher and Eyre 2010; Krause-Jensen and Duarte 2016). DOC exudation by benthic microalgae and ephemeral macroalgae, that would be present within the canopy as epiphytes on the fronds or as a biofilm on the underlying rocks, would also contribute to DOC export (Underwood and Paterson 2003). Based on these literature values, it is possible that the *F. vesiculosus* canopy investigated in this study exuded DOC at a rate of 37–73 mmol m^{-2} d^{-1} (0.5–0.9 g C m^{-2} d^{-1}) during peak production periods in summer, which is at the upper range of values reported for seagrass beds and macroalgae worldwide (Maher and Eyre 2010; Barrón et al. 2014). The derived annual values of DOC export from the *F. vesiculosus* canopy of 5–10 mol m^{-2} yr^{-1} (60–121 g C m^{-2} yr^{-1}) are in good agreement with the global average value for DOC export from algal beds of 8 mol m^{-2} yr^{-1} (101 g C m^{-2} yr^{-1}) (Krause-Jensen and Duarte 2016).

Outlook and perspectives

Decades after the influential studies by Mann (1973) and Smith (1981), the important functions of vegetated seafloor habitats in the oceanic C cycle are increasingly being recognized (Duarte 2017). Despite this advancement, the dynamics of macroalgal canopy productivity remain poorly understood. Recent technological developments, such as the AEC technique used in this study, as well as other non-invasive techniques that integrate over large seafloor surface areas (tens to hundreds of square meter) (Falter et al. 2008; McGillis et al. 2011), constitute promising new tools to investigate habitat-scale productivity rates and their drivers in macroalgal canopies under in situ conditions. The high temporal flux resolution that AEC provides enabled us to investigate hourly dynamics in detail. In this study, we have documented the importance of perennial macroalgal canopies in the Baltic Sea for primary productivity and biogeochemical functioning, on timescales ranging from 1 h to 1 yr. The *F. vesiculosus* canopy effected high hourly rates of oxygen production that are comparable to the most productive seagrass beds worldwide. Through detailed analyses of the hourly flux dynamics and their drivers, we were able to identify a mechanism that explains an apparent release of oxygen by the seafloor under dark conditions. The fact that high hourly rates of oxygen production were also measured in late winter under low light availability and cold water temperatures is a substantial new finding that highlights the importance of conducting seasonal measurements. The canopy was highly net autotrophic on an annual basis, and we are able to conclude, through comparing annual *NEM* with seasonal measurements of canopy standing biomass, that much of this surplus C production is exported to its surroundings.

Macroalgal canopies represent significantly understudied habitats when compared to other conspicuous canopy-forming vegetation such as seagrasses. More research is required to investigate *NEM* and its drivers within macroalgal canopies. Additional measurements in mid-winter (January), as well as during other periods of interest (e.g., storms and production blooms), would provide considerable new insight. Incorporating macrovegetation into estimates of coastal primary productivity is an important next step. Furthermore, determining the fate of the exported C from macroalgal canopies, and its importance as a resource subsidy for secondary production in adjacent seafloor communities, requires further research.

References

Aleem, A. A. 1969. Zonation, vesicle pressure and gas composition in *Fucus vesiculosus* and *Ascophyllum nodosum* at Kristineberg (west coast of Sweden). Mar. Biol. **4**: 36. doi:10.1007/BF00372164

Anderson, L. M., and P. T. Martone. 2014. Biomechanical consequences of epiphytism in intertidal macroalgae. J. Exp. Biol. **217**: 1167–1174. doi:10.1242/jeb.088955

Attard, K. M., R. N. Glud, D. F. McGinnis, and S. Rysgaard. 2014. Seasonal rates of benthic primary production in a Greenland fjord measured by aquatic eddy correlation. Limnol. Oceanogr. **59**: 1555–1569. doi:10.4319/lo.2014.59.5.1555

Attard, K. M., H. Stahl, N. A. Kamenos, G. Turner, H. L. Burdett, and R. N. Glud. 2015. Benthic oxygen exchange in a live coralline algal bed and an adjacent sandy habitat: An eddy covariance study. Mar. Ecol. Prog. Ser. **535**: 99–115. doi:10.3354/meps11413

Barrón, C., E. T. Apostolaki, and C. M. Duarte. 2014. Dissolved organic carbon fluxes by seagrass meadows and macroalgal beds. Front. Mar. Sci. **1**: 77. doi:10.3389/fmars.2014.00077

Berg, P., H. Røy, and P. L. Wiberg. 2007. Eddy correlation flux measurements: The sediment surface area that contributes to the flux. Limnol. Oceanogr. **52**: 1672–1684. doi:10.4319/lo.2007.52.4.1672

Berg, P., and M. Huettel. 2008. Monitoring the seafloor using the noninvasive eddy correlation technique: Integrated

benthic exchange dynamics. Oceanography **21**: 164–167. doi:10.5670/oceanog.2008.13

Berg, P. and others 2003. Oxygen uptake by aquatic sediments measured with a novel non-invasive eddy-correlation technique. Mar. Ecol. Prog. Ser. **261:** 75–83. doi:10.3354/meps261075

Berg, P. and others 2013. Eddy correlation measurements of oxygen fluxes in permeable sediments exposed to varying current flow and light. Limnol. Oceanogr. **58:** 1329–1343. doi:10.4319/lo.2013.58.4.1329

Bonsdorff, E. 1992. Drifting algae and zoobenthos—effects on settling and community structure. Neth. J. Sea Res. **30**: 57–62. doi:10.1016/0077-7579(92)90045-G

Bordeyne, F., A. Migne, and D. Davoult. 2017. Variation of fucoid community metabolism during the tidal cycle: Insights from *in situ* measurements of seasonal carbon fluxes during emersion and immersion. Limnol. Oceanogr. **62**: 2418–2430. doi:10.1002/lno.10574

Carlson, D. J., and M. L. Carlson. 1984. Reassessment of exudation by fucoid macroalgae. Limnol. Oceanogr. **29**: 1077–1087. doi:10.4319/lo.1984.29.5.1077

Charpy-Roubad, C., and A. Sournia. 1990. The comparative estimation of phytoplanktonic, microphytobenthic and macrophytobenthic primary production in the oceans. Mar. Microbial. Food Webs **4**: 31–57.

Chipman, L., P. Berg, and M. Huettel. 2016. Benthic oxygen fluxes measured by Eddy covariance in permeable Gulf of Mexico shallow-water sands. Aquatic Geochem. **22**: 529–554. doi:10.1007/s10498-016-9305-3

Damant, G. C. C. 1936. Storage of oxygen in the bladders of *Ascophyllum nodosum* and their adaptation to hydrostatic pressure. J. Exp. Biol. **14**: 198–209.

Dierssen, H. M., R. C. Zimmerman, L. A. Drake, and D. J. Burdige. 2009. Potential export of unattached benthic macroalgae to the deep sea through wind-driven Langmuir circulation. Geophys. Res. Lett. **36**: L04602. doi:10.1029/2008GL036188

Donis, D. and others 2015. An assessment of the precision and confidence of aquatic eddy correlation measurements. J. Atmos. Ocean Tech. **32**: 642–655. doi:10.1175/JTECH-D-14-00089.1

Duarte, C. M. 2017. Reviews and syntheses: Hidden forests, the role of vegetated coastal habitats in the ocean carbon budget. Biogeosciences **14**: 301–310. doi:10.5194/bg-14-301-2017

Duarte, C. M., and J. Cebrian. 1996. The fate of marine autotrophic production. Limnol. Oceanogr. **41**: 1758–1766. doi:10.4319/lo.1996.41.8.1758

Falter, J. L., R. J. Lowe, M. J. Atkinson, S. G. Monismith, and D. W. Schar. 2008. Continuous measurements of net production over a shallow reef community using a modified Eulerian approach. J. Geophys. Res.: Oceans **113**: C07035. doi:10.1029/2007JC004663

Fenchel, T., and R. N. Glud. 2000. Benthic primary production and O_2-CO_2 dynamics in a shallow-water sediment: Spatial and temporal heterogeneity. Ophelia **53**: 159–171.

Field, C. B., M. J. Behrenfeld, J. T. Randerson, and P. Falkowski. 1998. Primary production of the biosphere: Integrating terrestrial and oceanic components. Science **281**: 237–240. doi:10.1126/science.281.5374.237

Filbee-Dexter, K., and R. E. Scheibling. 2014. Sea urchin barrens as alternative stable states of collapsed kelp ecosystems. Mar. Ecol. Prog. Ser. **495**: 1–25. doi:10.3354/meps10573

Ganguly, D., G. Singh, P. Ramachandran, A. P. Selvam, K. Banerjee, and R. Ramachandran. 2017. Seagrass metabolism and carbon dynamics in a tropical coastal embayment. Ambio **46**: 667–679. doi:10.1007/s13280-017-0916-8

Gattuso, J. P., B. Gentili, C. M. Duarte, J. A. Kleypas, J. J. Middelburg, and D. Antoine. 2006. Light availability in the coastal ocean: Impact on the distribution of benthic photosynthetic organisms and their contribution to primary production. Biogeosciences **3**: 489–513. doi:10.5194/bg-3-489-2006

Glud, R. N., S. Rysgaard, T. Fenchel, and P. H. Nielsen. 2004. A conspicuous H2S-oxidizing microbial mat from a high-latitude Arctic fjord (young sound, NE Greenland). Mar. Biol. **145**: 51–60.

Glud, R. N. and others 2010. Benthic O_2 exchange across hard-bottom substrates quantified by eddy correlation in a sub-Arctic fjord. Mar. Ecol. Prog. Ser. **417:** 1–12. doi:10.3354/meps08795

Gruber, R. K., R. J. Lowe, and J. L. Falter. 2017. Metabolism of a tide-dominated reef platform subject to extreme diel temperature and oxygen variations. Limnol. Oceanogr. **62**: 1701–1717. doi:10.1002/lno.10527

Gundersen, J. K., N. B. Ramsing, and R. N. Glud. 1998. Predicting the signal of O_2 microsensors from physical dimensions, temperature, salinity, and O_2 concentration. Limnol. Oceanogr. **43**: 1932–1937. doi:10.4319/lo.1998.43.8.1932

Harrold, C., K. Light, and S. Lisin. 1998. Organic enrichment of submarine-canyon and continental-shelf benthic communities by macroalgal drift imported from nearshore kelp forests. Limnol. Oceanogr. **43**: 669–678. doi:10.4319/lo.1998.43.4.0669

Hendriks, I. E. and others 2014. Photosynthetic activity buffers ocean acidification in seagrass meadows. Biogeosciences **11:** 13.

Holtappels, M. and others 2013. Effects of transient bottom water currents and oxygen concentrations on benthic exchange rates as assessed by eddy correlation measurements. J. Geophys. Res.: Oceans **118:** 1157–1169. doi:10.1002/jgrc.20112

Holtappels, M. and others 2015. Aquatic eddy correlation: Quantifying the artificial flux caused by stirring-sensitive O_2 sensors. PLoS ONE **10**(1): e0116564. doi:10.1371/journal.pone.0116564

Hume, A. C., P. Berg, and K. J. McGlathery. 2011. Dissolved oxygen fluxes and ecosystem metabolism in an eelgrass

(*Zostera marina*) meadow measured with the eddy correlation technique. Limnol. Oceanogr. **56**: 86–96. doi:10.4319/lo.2011.56.1.0086

Hylleberg Kristensen, J. 1972. Carbohydrases of some marine invertebrates with notes on their food and on the natural occurrence of the carbohydrates studied. Mar. Biol. **14**: 130–142. doi:10.1007/BF00373212

Ilvessalo, H., and J. Tuomi. 1989. Nutrient availability and accumulation of phenolic-compounds in the brown alga *Fucus vesiculosus*. Mar. Biol. **101**: 115–119. doi:10.1007/BF00393484

Inoue, T., R. N. Glud, H. Stahl, and A. Hume. 2011. Comparison of three different methods for assessing in situ friction velocity: A case study from loch Etive, Scotland. Limnol. Oceanogr.: Methods **9**: 275–287. doi:10.4319/lom.2011.9.275

Kairesalo, T., and E. Leskinen. 1986. Measurements of metabolic activities within a Baltic *Fucus vesiculosus* community: The contribution of fouling microalgae and grazers, p. 301–312. *In* L. V. Evans and K. D. Hoagland [eds.], Studies in environmental science. Elsevier.

Kautsky, N., H. Kautsky, U. Kautsky, and M. Waern. 1986. Decreased depth penetration of *Fucus vesiculosus* (L) since the 1940s indicates eutrophication of the Baltic Sea. Mar. Ecol. Prog. Ser. **28**: 1–8. doi:10.3354/meps028001

Kiirikki, M., and A. Ruuskanen. 1996. How does *Fucus vesiculosus* survive ice scraping? Bot. Mar. **39**: 113–139.

Knight, M., and M. Parke. 1950. A biological study of *Fucus vesiculosus* L and *Fucus serratus* L. J. Mar. Biol. Assoc. UK **29**: 439–515.

Krause-Jensen, D., and C. M. Duarte. 2014. Expansion of vegetated coastal ecosystems in the future Arctic. Front. Mar. Sci. **1**: 77. doi:10.3389/fmars.2014.00077

Krause-Jensen, D., and C. M. Duarte. 2016. Substantial role of macroalgae in marine carbon sequestration. Nat. Geosci. **9**: 737–742. doi:10.1038/ngeo2790

Krumhansl, K. A., and R. E. Scheibling. 2012. Production and fate of kelp detritus. Mar. Ecol. Prog. Ser. **467**: 281–302. doi:10.3354/meps09940

Kuparinen, J., J. M. Leppanen, J. Sarvala, A. Sundberg, and A. Virtanen. 1984. Production and utilization of organic matter in a Baltic ecosystem off Tvärminne, southwest coast of Finland. Rapp. P.-V. Reun. Cons. Int. Explor. Mer. **183**: 180–192.

Lappalainen, A., M. Rask, H. Koponen, and S. Vesala. 2001. Relative abundance, diet and growth of perch (*Perca fluviatilis*) and roach (*Rutilus rutilus*) at Tvärminne, northern Baltic Sea, in 1975 and 1997: Responses to eutrophication? Boreal Environ. Res. **6**: 107–118.

Lee, J. S. and others 2017. Estimation of net ecosystem metabolism of seagrass meadows in the coastal waters of the East Sea and Black Sea using the noninvasive eddy covariance technique. Ocean Sci. J. **52:** 243–256. doi:10.1007/s12601-017-0032-5

Leskinen, E., A. Mäkinen, W. Fortelius, M. Lindström, and H. Salemaa. 1992. Primary production of macroalgae in relation to the spectral range and sublittoral light conditions in the Tvärminne archipelago, northern Baltic Sea. Acta Phytogeogr. Suec. **78**: 85–93.

Lignell, R. and others 1993. Fate of a phytoplankton spring bloom—sedimentation and carbon flow in the planktonic food web in the northern Baltic. Mar. Ecol. Prog. Ser. **94:** 239–252. doi:10.3354/meps094239

Long, M. H., P. Berg, D. de Beer, and J. C. Zieman. 2013. *In situ* coral reef oxygen metabolism: An eddy correlation study. PLoS ONE **8**(3): e58581. doi:10.1371/journal.pone.0058581

Long, M. H., P. Berg, and J. L. Falter. 2015*a*. Seagrass metabolism across a productivity gradient using the eddy covariance, Eulerian control volume, and biomass addition techniques. J. Geophys. Res.: Oceans **120**: 3624–3639.

Long, M. H., P. Berg, K. J. McGlathery, and J. C. Zieman. 2015*b*. Sub-tropical seagrass ecosystem metabolism measured by eddy covariance. Mar. Ecol. Prog. Ser. **529**: 75–90.

Lorke, A., D. F. McGinnis, and A. Maeck. 2013. Eddy-correlation measurements of benthic fluxes under complex flow conditions: Effects of coordinate transformations and averaging time scales. Limnol. Oceanogr.: Methods **11**: 425–437.

Lorrai, C., D. F. McGinnis, P. Berg, A. Brand, and A. Wuest. 2010. Application of oxygen eddy correlation in aquatic systems. J. Atmos. Ocean Tech. **27**: 1533–1546. doi:10.1175/2010JTECHO723.1

Maher, D. T., and B. D. Eyre. 2010. Benthic fluxes of dissolved organic carbon in three temperate Australian estuaries: Implications for global estimates of benthic DOC fluxes. J. Geophys. Res.: Biogeosci. **115**: G04039. doi:10.1029/2010JG001433

Mann, K. H. 1973. Seaweeds—their productivity and strategy for growth. Science **182**: 975–981. doi:10.1126/science.182.4116.975

Markager, S., and K. Sand-Jensen. 1992. Light requirements and depth zonation of marine macroalgae. Mar. Ecol. Prog. Ser. **88**: 83–92. doi:10.3354/meps088083

Martin, S., J. Clavier, L. Chauvaud, and G. Thouzeau. 2007. Community metabolism in temperate maerl beds. I. Carbon and carbonate fluxes. Mar. Ecol. Prog. Ser. **335**: 19–29. doi:10.3354/meps335019

Martin, S. and others 2005. Comparison of Zostera marina and maerl community metabolism. Aquat. Bot. **83:** 161–174. doi:10.1016/j.aquabot.2005.06.002

Mass, T., A. Genin, U. Shavit, M. Grinstein, and D. Tchernov. 2010. Flow enhances photosynthesis in marine benthic autotrophs by increasing the efflux of oxygen from the organism to the water. Proc. Natl. Acad. Sci. USA **107**: 2527–2531.

McGillis, W. R., C. Langdon, B. Loose, K. K. Yates, and J. Corredor. 2011. Productivity of a coral reef using boundary layer and enclosure methods. Geophys. Res. Lett. **38**: L03611. doi:10.1029/2010GL046179

McGinnis, D. F., P. Berg, A. Brand, C. Lorrai, T. J. Edmonds, and A. Wuest. 2008. Measurements of eddy correlation oxygen fluxes in shallow freshwaters: Towards routine applications and analysis. Geophys. Res. Lett. **35**: L04403. doi:10.1029/2007GL032747

McGinnis, D. F. and others 2011. Simple, robust eddy correlation amplifier for aquatic dissolved oxygen and hydrogen sulfide flux measurements. Limnol. Oceanogr.: Methods **9:** 340–347. doi:10.4319/lom.2011.9.340

Sieburth, J. M. N. 1969. Studies on the algal substances in the sea. III. The production of extracellular organic matter by littoral marine algae. J. Exp. Mar. Biol. Ecol. **3**: 290–309.

Moriarty, D. J. W., D. G. Roberts, and P. C. Pollard. 1990. Primary and bacterial productivity of tropical seagrass communities in the Gulf of Carpentaria, Australia. Mar. Ecol. Prog. Ser. **61**: 145–157. doi:10.3354/meps061145

Norkko, A., and E. Bonsdorff. 1996. Population responses of coastal zoobenthos to stress induced by drifting algal mats. Mar. Ecol. Prog. Ser. **140**: 141–151. doi:10.3354/meps140141

Norkko, J., E. Bonsdorff, and A. Norkko. 2000. Drifting algal mats as an alternative habitat for benthic invertebrates: Species specific responses to a transient resource. J. Exp. Mar. Biol. Ecol. **248**: 79–104. doi:10.1016/S0022-0981(00)00155-6

Norkko, A., A. Villnäs, J. Norkko, S. Valanko, and C. Pilditch. 2013. Size matters: Implications of the loss of large individuals for ecosystem function. Sci. Rep.-Uk **3**: 2646. doi:10.1038/srep02646

Olivé, I., J. Silva, M. M. Costa, and R. Santos. 2016. Estimating seagrass community metabolism using benthic chambers: The effect of incubation time. Estuar. Coasts **39**: 138–144. doi:10.1007/s12237-015-9973-z

Polis, G. A., W. B. Anderson, and R. D. Holt. 1997. Toward an integration of landscape and food web ecology: The dynamics of spatially subsidized food webs. Annu. Rev. Ecol. Syst. **28**: 289–316. doi:10.1146/annurev.ecolsys.28.1.289

Pollard, P. C., and D. J. W. Moriarty. 1991. Organic carbon decomposition, primary and bacterial productivity, and sulfate reduction, in tropical seagrass beds of the Gulf of Carpentaria, Australia. Mar. Ecol. Prog. Ser. **69**: 149–159. doi:10.3354/meps069149

Råberg, S., and L. Kautsky. 2007. A comparative biodiversity study of the associated fauna of perennial fucoids and filamentous algae. Estuar. Coast. Shelf Sci. **73**: 249–258. doi:10.1016/j.ecss.2007.01.005

Reimers, C. E., H. T. Ozkan-Haller, P. Berg, A. Devol, K. McCann-Grosvenor, and R. D. Sanders. 2012. Benthic oxygen consumption rates during hypoxic conditions on the Oregon continental shelf: Evaluation of the eddy correlation method. J. Geophys. Res.: Oceans **117**: C02021. doi:10.1029/2011JC007564x

Revsbech, N. P. 1989. An oxygen microsensor with a guard cathode. Limnol. Oceanogr. **34**: 474–478. doi:10.4319/lo.1989.34.2.0474

Rheuban, J. E., and P. Berg. 2013. The effects of spatial and temporal variability at the sediment surface on aquatic eddy correlation flux measurements. Limnol. Oceanogr.: Methods **11**: 351–359.

Rheuban, J. E., P. Berg, and K. J. McGlathery. 2014*a*. Ecosystem metabolism along a colonization gradient of eelgrass (*Zostera marina*) measured by eddy correlation. Limnol. Oceanogr. **59**: 1376–1387.

Rheuban, J. E., P. Berg, and K. J. McGlathery. 2014*b*. Multiple timescale processes drive ecosystem metabolism in eelgrass (*Zostera marina*) meadows. Mar. Ecol. Prog. Ser. **507**: 1–13.

Rohde, S., M. Molis, and M. Wahl. 2004. Regulation of antiherbivore defence by *Fucus vesiculosus* in response to various cues. J. Ecol. **92**: 1011–1018. doi:10.1111/j.0022-0477.2004.00936.x

Russell, G. 1985. Recent evolutionary changes in the algae of the Baltic Sea. Brit. Phycol. J. **20**: 87–104.

Smith, S. V. 1981. Marine macrophytes as a global carbon sink. Science **211**: 838–840. doi:10.1126/science.211.4484.838

Sorrell, B. K., and F. I. Dromgoole. 1986. Errors in measurements of aquatic macrophyte gas-exchange due to oxygen storage in internal airspaces. Aquat. Bot. **24**: 103–114. doi:10.1016/0304-3770(86)90091-4

Tait, L. W., and D. R. Schiel. 2010. Primary productivity of intertidal macroalgal assemblages: Comparison of laboratory and in situ photorespirometry. Mar. Ecol. Prog. Ser. **416**: 115–125. doi:10.3354/meps08781

Tammes, P. M. L. 1954. Gas-exchange in the vesicles (air bladders) of *Ascophyllum nodosum*. Acta Bot. Neerl. **3**: 114–123. doi:10.1111/j.1438-8677.1954.tb00291.x

Torn, K., D. Krause-Jensen, and G. Martin. 2006. Present and past depth distribution of bladderwrack (*Fucus vesiculosus*) in the Baltic Sea. Aquat. Bot. **84**: 53–62. doi:10.1016/j.aquabot.2005.07.011

Underwood, G. J. C., and D. M. Paterson. 2003. The importance of extracellular carbohydrate production by marine epipelic diatoms, p. 183–240. *In* J. A. Callow [ed.], Advances in botanical research. Academic.

Vallance, K. B., and D. A. Coult. 1951. Observations on the gaseous exchanges which take place between Menyanthes-Trifoliata L and its environment. 1. The composition of the internal gas of the plant. J. Exp. Bot. **2**: 212–222. doi:10.1093/jxb/2.2.212

Vetter, E. W. 1994. Hotspots of benthic production. Nature **372**: 47–47. doi:10.1038/372047a0

Wada, S., and T. Hama. 2013. The contribution of macroalgae to the coastal dissolved organic matter pool. Estuar. Coast. Shelf Sci. **129**: 77–85. doi:10.1016/j.ecss.2013.06.007

Walpersdorf, E. and others 2017. In situ oxygen dynamics and carbon turnover in an intertidal sediment (Skallingen,

Denmark). Mar. Ecol. Prog. Ser. **566:** 49–65. doi:10.3354/meps12016

Wüest, A., and A. Lorke. 2003. Small-scale hydrodynamics in lakes. Annu. Rev. Fluid Mech. **35**: 373–412. doi:10.1146/annurev.fluid.35.101101.161220

Zieman, J. C. 1974. Methods for the study of the growth and production of turtle grass, *Thalassia testudinum* König. Aquaculture **4**: 139–143. doi:10.1016/0044-8486(74)90029-5

Acknowledgments

The authors are grateful for the help they received for this project from colleagues at the Tvärminne Zoological Station. In particular, the authors acknowledge Mats Westerbom, Veijo Kinnunen, Hanna Halonen, Göran Lundberg, and the Benthic Ecology team for their help with planning and logistics. The authors are grateful to Anni Glud and Morten Larsen at the University of Southern Denmark for constructing the oxygen microsensors used in this study. The Walter and Andrée de Nottbeck Foundation supported this work through a postdoctoral fellowship to K.M.A. and through a senior research fellowship to R.N.G. Further funding for this project was provided by research grants from The Academy of Finland (project ID 294853), the University of Helsinki and Stockholm University strategic fund for collaborative research, the European Commission through HADES-ERC (project ID 669947) and ATLAS (project ID 678760), the Danish National Research Council (FNU 7014-00078), and the U.S. National Science Foundation (OCE-1061364 and OCE-1334848).

Conflict of Interest

None declared.

Submitted 15 March 2018
Revised 13 June 2018
Accepted 30 July 2018

Associate editor: Núria Marbà